Arch Toxicol (2016) 90:3029–3044
DOI 10.1007/s00204-016-1659-1

IN VITRO SYSTEMS

Toxicity of wood smoke particles in human A549 lung epithelial cells: the role of PAHs, soot and zinc

Marco Dilger[1] · Jürgen Orasche[2] · Ralf Zimmermann[2,3] · Hanns-Rudolf Paur[4] · Silvia Diabaté[1] · Carsten Weiss[1]

Received: 11 May 2015 / Accepted: 4 January 2016 / Published online: 2 February 2016

Abstract Indoor air pollution is associated with increased morbidity and mortality. Specifically, the health impact of emissions from domestic burning of biomass and coal is most relevant and is estimated to contribute to over 4 million premature deaths per year worldwide. Wood is the main fuel source for biomass combustion and the shift towards renewable energy sources will further increase emissions from wood combustion even in developed countries. However, little is known about the constituents of wood smoke and biological mechanisms that are responsible for adverse health effects. We exposed A549 lung epithelial cells to collected wood smoke particles and found an increase in cellular reactive oxygen species as well as a response to bioavailable polycyclic aromatic hydrocarbons. In contrast, cell vitality and regulation of the pro-inflammatory cytokine interleukin-8 were not affected. Using a candidate approach, we could recapitulate WSP toxicity by the combined actions of its constituents soot, metals and PAHs. The soot fraction and metals were found to be the most important factors for ROS formation, whereas the PAH response can be mimicked by the model PAH benzo[a]pyrene. Strikingly, PAHs adsorbed to WSPs were even more potent in activating target gene expression than B[a]P individually applied in suspension. As PAHs initiate multiple adverse outcome pathways and are prominent carcinogens, their role as key pollutants in wood smoke and its health effects warrants further investigation. The presented results suggest that each of the investigated constituents soot, metals and PAHs are major contributors to WSP toxicity. Mitigation strategies to prevent adverse health effects of wood combustion should therefore not only aim at reducing the emitted soot and PAHs but also the metal content, through the use of more efficient combustion appliances, and particle precipitation techniques, respectively.

Keywords Wood smoke · Particulate matter · Lung epithelial cells · Polycyclic aromatic hydrocarbons · Soot · Metals

Electronic supplementary material The online version of this article (doi:10.1007/s00204-016-1659-1) contains supplementary material, which is available to authorized users.

✉ Carsten Weiss
carsten.weiss@kit.edu

[1] Karlsruhe Institute of Technology, Campus North, Institute of Toxicology and Genetics, Hermann-von-Helmholtz-Platz 1, 76344 Eggenstein-Leopoldshafen, Germany

[2] Joint Mass Spectrometry Centre—Comprehensive Molecular Analytics, Helmholtz Zentrum München, Ingolstädter Landstraße 1, D-85764 Neuherberg, Germany

[3] Joint Mass Spectrometry Centre—Chair of Analytical Chemistry, Institute of Chemistry, University of Rostock, Dr.-Lorenz-Weg 1, 18051 Rostock, Germany

[4] Karlsruhe Institute of Technology, Campus North, Institute for Technical Chemistry, Hermann-von-Helmholtz-Platz 1, 76344 Eggenstein-Leopoldshafen, Germany

Introduction

Worldwide, around one-third of the human population relies daily on the burning of biomass (e.g. wood and crop residues) and coal for heating and cooking (Bonjour et al. 2013). In the recent years, the emissions from burning these fuels have gained attention as an important source of adverse health effects. The WHO estimates over 4 million premature deaths annually attributable to domestic burning of biomass and coal (World Health Organization 2014).

Human exposure to combustion products from biomass and coal is particularly prevalent in developing countries,

where solid fuel is often used indoors without proper ventilation. In higher-income countries, less domestic burning of solid fuels and better ventilation usually leads to a lower indoor exposure. But even in these countries, 10–15 % of ambient particulate matter originates from biomass combustion (Thurston et al. 2011; Belis et al. 2013).

Wood is the main fuel source for domestic biomass combustion (Straif et al. 2013), and wood smoke has recently emerged as a major health concern (Naeher et al. 2007; Kocbach Bølling et al. 2009). While the association of ambient particulate matter (PM) with adverse health effects has long been established (Dockery and Pope 1994), much less research has been devoted to the impact of wood combustion.

Epidemiological studies repeatedly link wood smoke emissions to increased morbidity and mortality, for example, in areas affected by wildfires (Johnston et al. 2012) and populations with high use of wood as a fuel source (Ezzati et al. 2000; Sanhueza et al. 2009). Further, pulmonary and systemic symptoms along with increased levels of urinary exposure markers could be found for workers with high occupational exposure (Kato et al. 2004; Swiston et al. 2008; Neitzel et al. 2009; Greven et al. 2012).

Recent short-term exposure studies in healthy volunteers or subjects with mild disease partially corroborate adverse health effects in humans (Janssen et al. 2012). However, although some studies find weak increases in pulmonary and systemic markers of inflammation (Riddervold et al. 2012; Ghio et al. 2012), other studies report no or very mild effects (Sehlstedt et al. 2010; Forchhammer et al. 2012; Stockfelt et al. 2012, 2013; Bønløkke et al. 2014; Jensen et al. 2014). Long-term exposure studies under controlled conditions are not possible with humans, but have been performed to a limited extent with rodents. As summarized by Naeher et al., these long-term studies on adverse health effects generally lend support to epidemiological data, but interspecies comparisons need to be approached with caution (Naeher et al. 2007).

In vitro studies with collected particles reduce the experimental complexity in comparison with in vivo studies, allowing for a more detailed focus on the molecular mechanism of action and the physicochemical parameters determining the toxicological outcome of wood smoke particle (WSP) exposure. The combustion of wood generates particulate matter consisting of a complex mixture of different chemical species (Schmidl et al. 2008; Orasche et al. 2013). Among these are potentially toxic compounds such as polycyclic aromatic hydrocarbons (PAHs) and soot, formed during incomplete combustion, as well as metals, which evaporate during the combustion process and condensate in lower-temperature zones.

Some PAHs are human carcinogens with well-documented mechanisms of action (Baird et al. 2005). Uski et al. found that particles collected during intermediate and smouldering combustion contain more PAHs than particles from efficient combustion which correlated with genotoxicity but not cytotoxicity or oxidative stress in murine macrophages (Uski et al. 2014). Kocbach et al. investigated the effects of collected WSPs from different combustion conditions on a co-culture model. Interestingly, although secretion of inflammatory cytokines was differentially induced by the organic fractions of particle extracts, this effect could not directly be correlated with PAH content (Bølling et al. 2012). Other researchers, however, reported PAH-mediated effects of particles originating from complete combustion which might be explained by a higher PAH bioavailability compared to the previous studies (Gauggel-Lewandowski et al. 2013). Increased levels of PAHs are often paralleled by enhanced soot content, depending on the combustion conditions, yet the role of soot for WSP toxicity is poorly understood. Several studies report a correlation between soot content and oxidative stress for other combustion-derived particles (Garza et al. 2008; Chuang et al. 2011). Surface area of the soot particles plays an important role in reactive oxygen species (ROS) formation (Nel et al. 2006; Stoeger et al. 2009). Carbon black, consisting of relatively pure elementary carbon, was occasionally used as a soot surrogate and induced both inflammation and ROS (Pulskamp et al. 2007; Aam and Fonnum 2007; Monteiller et al. 2007; Garza et al. 2008; Diabaté et al. 2011).

In contrast to PAHs and soot, trace metals are enriched in the particulate phase at higher combustion temperatures. Emissions of inorganic particles containing trace metals may shift the toxicity profile and metal emissions appear to be particularly high when the metal content is reported relative to total particle mass, a common practice in particle toxicology. Many metal compounds (i.e. the respective salts and oxides) are well known for their cytotoxic and carcinogenic properties (Stohs and Bagchi 1995; Beyersmann and Hartwig 2008) and have been implicated in toxicity induced by combustion-derived particles (Fritsch-Decker et al. 2011; Diabaté et al. 2011). WSPs with high metal content triggered more acute toxicity and ROS formation compared to other WSPs in rat macrophages (Uski et al. 2014). Zinc is usually the predominant trace metal in WSPs. Zinc oxide nanoparticles and zinc containing artificial reference particles were tested in comparison with WSPs and could reproduce WSP toxicity to some extent (Torvela et al. 2014b).

In order to reduce adverse health effects associated with wood combustion, primary and secondary measures to control emissions have to be implemented. For example, in Germany stringent legislation has been passed to reduce particulate emissions (BImSchG 2014). Improved stoves and boilers providing more efficient combustion conditions reduce the products of incomplete combustion (Johansson

et al. 2004). Indeed, such measures have already proven successful in rural areas (McCracken et al. 2007; Noonan et al. 2012) but may shift the profile of toxicity due to elevated metal emissions as described above. Therefore, a reduction of particulate emissions, including metal species, would be desirable, e.g. by the use of electrostatic precipitation (Bologa et al. 2011; Pudasainee et al. 2014). These measures are feasible for small-scale wood combustion boilers (25–500 kW). However, for even smaller log-wood stoves, such as those used in large numbers for residential wood combustion, further strategies need to be explored. Hence, identification of key constituents of WSPs driving adverse effects is instrumental and ultimately will serve regulatory purposes to establish appropriate dose metrics and potential thresholds, which are currently mostly based on emitted PM mass (Cassee et al. 2013).

In vitro toxicity testing of collected WSPs is a valuable tool in this process. By the use of a candidate approach, critical constituents of WSPs can be assessed individually to identify the most relevant driver(s) of toxicity. In this study, we applied WSPs collected from wood combustion in a domestic stove to human lung epithelial cells (A549) and addressed several toxicological endpoints, i.e. acute toxicity, response to bioavailable PAHs, inflammation and oxidative stress. Our hypothesis was that the toxicity of the complex mixture of WSPs can be reproduced by some of its constituents. To this end, we chose the model PAH benzo[a]pyrene (B[a]P), carbon black nanoparticles (CB14, Printex 90®) and zinc oxide nanoparticles (ZnO) to represent the PAH, soot and metal fraction of WSPs, respectively.

Methods

Materials and reagents

Materials and reagents were obtained from the following suppliers: Foetal calf serum (FCS): PAA Laboratories (Cölbe, Germany). Medium, supplements and other reagents used for cell culture; 2′,7′-dichlorodihydrofluorescein-diacetate ($DCFH_2$-DA); phosphate-buffered saline without calcium and magnesium (PBS): Invitrogen, (Karlsruhe, Germany). Chromogenic Limulus Amebocyte Lysate (LAL) assay: Lonza (Basel, Switzerland). MSTFA (N-Methyl-N-trimethylsilyl-trifluoroacetamide): Macherey–Nagel (Düren, Germany). Cytotoxicity detection kit based on release of lactate dehydrogenase (LDH): Roche (Mannheim, Germany). AlamarBlue® reagent for viability testing: AbD Serotec (Puchheim, Germany). OptEIA ELISA kit: BD Biosciences (Heidelberg, Germany). peqGold TriFast (Trizol): Peqlab (Erlangen, Germany). DNAse (RQ1 RNase-Free DNase); reverse transcriptase (M-MLV RT (H-) Point mutant); dNTP mix: Promega, (Mannheim, Germany). Primers were synthesized by Metabion, Planegg-Martinsried, Germany. RNAse inhibitor (RiboLock); DNA polymerase (DreamTaq): Fermentas (St. Leon-Rot, Germany). SYBR QuantiTect Green PCR mastermix: Qiagen (Hilden, Germany). Odyssey blocking reagent and secondary IRDye™ antibodies for Western blots: LICOR Biosciences (Bad Homburg, Germany). Primary antibodies: Santa Cruz Biotechnology (Heidelberg, Germany). Benzo[a]pyrene, with a purity of >99 % as determined by GC–MS, was purchased from the Biochemical Institute for Environmental Carcinogens, Grosshansdorf, Germany. 7-ethoxyresorufin: Cayman Chemical (Ann Arbour, MI), Deferoxaminemesylate: Sigma-Aldrich (Taufkirchen, Germany), cadmium oxide (CdO): Merck (Darmstadt, Germany). All other, not specifically mentioned chemicals were purchased from Roth (Karlsruhe, Germany).

Particles and preparation of suspensions and reference substances

The WSPs were collected from emissions during a field study by the Technologie- und Förderzentrum (TFZ) Straubing, Germany, using a common tiled stove operated in a private household. Corresponding to prevailing habits of wood combustion in the private sector, the particles were collected under incomplete combustion conditions using mixed fuel. The fuel consisted of wood briquettes, split logs comprised of hard and soft wood, as well as waste wood. The particles were characterized by Gauggel et al. (sample "PM#2") (Gauggel et al. 2012) and kindly provided by Sonja Mülhopt (Karlsruhe Institute of Technology, Germany). The nano-sized carbon black particles (CB14, Printex®90) were kindly provided by Evonik (Frankfurt, Germany), and the ZnO nanomaterial (<100 nm) was purchased from Sigma-Aldrich (Cat.nr. 54906, Taufkirchen, Germany). For cell exposure experiments, stock suspensions of 1 mg/mL in cell culture medium were prepared from 5 to 15 mg of particles. The stock suspensions were probe sonified for 15 s (duty cycle 50, output control 5, Branson Sonifier, 250, Schwäbisch Gmünd, Germany) and diluted in cell culture medium. Please note that a probe sonifier delivers more energy to the sample than a sonication bath, for which longer sonication times would be appropriate. All experiments in this study were performed in the absence of serum. Serum-free conditions were chosen because adsorption of proteins can change the physicochemical properties of particles with implications for their in vitro toxicity (Panas et al. 2013). In the lung, the main exposure route for WSPs, particles are not coated with serum proteins and can directly interact with the tissue. For TEM analysis and the CdO nanoparticles stock suspension,

ultrapure water was used for dispersion. A benzo[a]pyrene (B[a]P) stock solution of 1 mM in DMSO was diluted in cell culture medium to prepare the solutions for B[a]P treatment. All particles were tested for endotoxin contamination with the LAL assay. Particle suspensions of 1 mg/mL in deionised water were centrifuged at 20,800 g for 10 min, and the supernatants were tested according to the instructions of the manufacturer. The result for each particle type was not distinguishable from the blank made from ultrapure water. It was therefore excluded that endotoxins contributed to the biological responses.

Chemical analysis of particulate matter

For analysis of particulate matter, extraction was carried out separately for non-polar and polar compounds with dichloromethane (GC ultra grade) and toluene (GC ultra grade), respectively, in an ultrasonic bath. Prior to extraction, approximately 10 mg of samples was spiked with internal standard mixtures as previously described (Orasche et al. 2011) and listed in the Supplementary Table S1. Ultra-sonication was carried out three times, each with two millilitres of solvent for fifteen minutes. The three extracts were combined and filtered over PTFE syringe membrane filters (0.2 µm, Sartorius, Germany). Dichloromethane extracts were evaporated to dryness. Derivatization was started by adding 100 µL of N-Methyl-N-(trimethylsilyl) trifluoroacetamide to the samples. Reaction time was 3 h at 80 °C. After derivatization, samples were injected to the GC–MS system (Shimadzu GCMS-QP2010 Ultra, Shimadzu, Japan). Toluene extracts were concentrated to 100 µL and directly injected to the GC, which was equipped with a 60 m BPX-5 column (0.22 mm ID, 0.25 µm film, SGE, Australia). A calibration was done by using the same set of internal standards and procedures (except ultra-sonication and filtration). Relative standard deviations of the procedure (RSD) were calculated via the confidence intervals.

Transmission electron microscopy (TEM)

Ten microlitres of particle suspensions at 50 µg/mL in deionized water was spotted on 75-mesh formvar-coated copper grids, dried at room temperature and observed with a Zeiss EM 109 T transmission electron microscope (Oberkochen, Germany).

Cell culture

The human alveolar epithelial cell line A549 was obtained from American Type Culture Collection (ATCC, Rockville, MD, USA) and maintained in Roswell Park Memorial Institute medium 1640 (RPMI) supplemented with 10 % (v/v) FCS, 100 U/mL penicillin, and 100 mg/mL streptomycin in 5 % CO_2 at 37 °C. The cells were passaged every 2 to 3 days before reaching confluence.

Toxicity test (LDH release)

1.65×10^5 A549 cells per well of a 24-well plate were seeded one day before the experiment. After treatment (600 µL per well), medium from the supernatant was collected and an aliquot (100 µL) was used for quantification of released LDH, an indicator of plasma membrane integrity. The LDH assay was performed in accordance with the manufacturer's instructions with slight modifications: the dye solution was diluted 1:1 (v/v) with PBS to slow down the reaction due to the high cell densities. The absorbance of the reaction mix was measured at 490 nm with a microplate reader, and values were analysed by the software package SoftMaxPro (Molecular Devices, Ismaning, Germany). Cell free medium, kept under the same conditions as the tested cells, was used to generate blank values, which were subsequently subtracted from all samples. Non-treated control cells were lysed with 0.1 to 1 % Triton X-100 for 30 min prior to the end of the experiments to obtain reference values for the highest LDH release achievable, and the measured values were set as 100 % toxicity.

Viability test (AlamarBlue®)

For testing the metabolic activity, A549 cells were seeded and treated as described for toxicity testing (LDH release). After treatment, the supernatant medium was replaced by AlamarBlue® diluted 1:10 (v/v) in RPMI 1640 without FCS supplementation, and the cells were incubated at 37 °C and 5 % CO_2 for 1 h. The AlamarBlue assay measures the ability of the cells to reduce the non-fluorescent dye resazurin to the fluorescent product resorufin by mitochondrial dehydrogenases (O'Brien et al. 2000); 100 µL of the supernatant was transferred to 96-well plates, and the fluorescence of the metabolically reduced reagent was quantified with a microplate reader (Bio-Tek FL600, software package KC4, MWG-Biotech AG, Ebersberg, Germany) at 580-nm excitation and 620-nm emission. AlamarBlue® diluted in medium without contact to cells was used as a blank. Blank values were subtracted from all samples and the fluorescence intensities of the samples were normalized to the untreated controls, which were set to 100 %.

Enzyme-linked immunosorbent assay (ELISA)

Secreted IL-8 was analysed from the supernatants of experiments performed as described for toxicity testing (LDH release) using OptEIA ELISA kits according to the manufacturer's instructions. For measurement of absorption and data analysis, a microplate reader and the software package

SoftMaxPro (Molecular Devices, Ismaning, Germany) were used.

ROS formation (DCF assay)

A549 cells were seeded in 96-well plates 1 day before the experiment, at a density of 3×10^4 cells/well. After 3 h incubation with 100 µL of particle suspensions per well, H_2DCF oxidation was measured as described before (Panas et al. 2013). The assay plates were handled in the absence of artificial light until reading. The metal chelator deferoxaminemesylate (DFO) was used in order to reduce metal-associated ROS formation (Fritsch-Decker et al. 2011; Diabaté et al. 2011). For these experiments, cells were pre-incubated for 15 min with 50 µL of 10 mM DFO or medium only; before 50 µL of twofold concentrated particle solutions were added for the indicated exposure time. The final DFO concentration was 5 mM.

Quantitative RT-PCR measurements of mRNA expression levels

One day before particle treatment, 3.35×10^5 A549 cells per well of a 12-well plate were seeded. Directly after treatment, in a volume of 1.22 mL per well, cells were lysed with 500 µL trizol reagent. Total RNA was extracted according to the manufacturer's instructions and dissolved in 30–50 µL of diethylpyrocarbonate-treated H_2O. Purity and concentration of the mRNA was measured spectrometrically (NanoDrop 1000U, Thermo Scientific, Wilmington, DE, USA); 0.5–1 µg mRNA was then treated with DNAse and reverse-transcribed with 200 U reverse transcriptase in a total reaction volume of 22 µL containing 91 µM of each dNTP, 200 ng of random hexanucleotide primers and 40 U RNAse inhibitor according to the supplier's protocol. To rule out a contamination with genomic DNA, additional sample aliquots were subjected to the transcription protocol in the absence of reverse transcriptase and checked for any polymerase activity by agarose gel electrophoresis and ethidiumbromide detection. Quantitative RT-PCR was performed in 20-µL reactions containing 10 µL 2 × Quantitect SYBR Green mastermix and 10 pmol primer pairs in an ABI StepOnePlus System (Applied Biosystems, Carlsbad, CA, USA) using the following conditions: 15-min activation at 95 °C, 40 amplification cycles (15-s denaturation at 95 °C, 30-s hybridization and elongation at 60 °C. The relative expression values of target mRNA were analysed using the $2^{-(\mathrm{ddCt})}$ method (Schmittgen and Livak 2008) with normalization to the reference gene large ribosomal protein P0 (RPLP0) using the following primer sequences (gene, forward, reverse): RPLP0, 5′-GAAGGCTGTGGTGCTGATGG-3′, 5′-CCGGATATGAGGCAGCAG-3′; CYP 1A1, 5′-GAGCCTCATGTATTTGGTGATG-3′, 5′-TTGTG TCTCTTGTTGTGCTGTG-3′ (Val et al. 2011); IL-8, 5′-GAATGGGTTTGCTAGAATGTGATA-3′,5′-CAG ACTAGGGTTGCCAGATTTAAC-3′; HO-1, 5′-TTCTCC GATGGGTCCTTACACT-3′, 5′-GGCATAAAGCCCTACA GCAACT-3′.

CYP1A1 activity (EROD assay)

The cells were seeded in 96-well plates and treated as described for the DCF assay. After 48 h, the supernatant medium was replaced by 100 µL of 8 µM 7-ethoxyresorufin (7-ER) in RPMI-1640 medium without phenol red in the absence of artificial light. After 30 min, the fluorescence was measured as described for the AlamarBlue® assay. Background fluorescence of 8 µM 7-ER was subtracted from all samples.

Heme oxygenase expression levels (Western blot)

For the analysis of protein expression, the cells were seeded into six-well plates at a density of 8.25×10^5 per well 24 h before the experiment. Cells were then treated for 24 h with the particles suspended in serum-free medium at the indicated concentrations. At the end of the exposure period, the medium was removed and the cells were lysed using 2× Laemmli buffer (125 mM Tris–HCl, 4 % SDS, 20 % glycerol, 8 % beta-mercaptoethanol, pH 6.8). Cell lysates were boiled at 95 °C for 5 min and sonicated in an ultrasonic bath for 10 min (Bandelin Sonorex, Berlin, Germany). Equal protein amounts were loaded on a 12 % gel for SDS-PAGE. After electrophoresis, the proteins were transferred onto an Immobilon-P membrane (Millipore, Eschborn, Germany). The membranes were blocked with Odyssey blocking buffer for 1 h and then incubated overnight at 4 °C with the primary antibodies against heme oxygenase 1 (sc-10789, Santa Cruz, diluted 1:1000) and Lamin B (sc-6216, Santa Cruz, diluted 1:2000) in a 1:1 (v/v) mixture of Odyssey Blocking Buffer and Tris-buffered saline containing 0.1 % Tween 20 (TBS-T). After washing, the membranes were incubated with the appropriate secondary IRDye™ 700 or 800 antibody 1:5000 diluted in the same buffer as the primary antibodies. Membranes were scanned using the Odyssey® Classic Infrared Imaging System (LICOR Biosciences). Image processing and quantification was done using Image Studio Lite 4.0 (LICOR Biosciences) with automated background correction (settings: median, width 5, all segments).

Statistical analysis

Values are reported as mean + standard deviation (SD) of multiple independent experiments except when otherwise indicated in the figure legends. Statistical analyses were

performed using R version 3.1.3 (R Foundation for Statistical Computing, Vienna, Austria). P values were calculated using analysis of variance (ANOVA) and Dunnett's post hoc test ("multicomp" package), using the respective controls as reference levels if not otherwise indicated. Values of $p < 0.05$ were considered statistically significant and annotated as indicated in the figure legends.

Results

Particle characterization

TEM was used to study the size distribution, morphology and agglomeration state of the tested particles (Fig. 1). The wood smoke particles (WSPs) are comprised of spherical primary particles with a size of about 20–40 nm, which are heavily agglomerated. Even after sonication, WSP agglomerates reach up to a few microns in diameter. Areas of crystalline structure were occasionally visible in proximity to WSPs, indicating the presence of inorganic salts that were dissolved and released from the WSPs by the dispersion process and precipitated on the TEM grids during drying. Carbon black nanoparticles (CB14) also show a spherical primary particle shape in the size range of 10–20 nm and also form large agglomerates, comparable to the WSPs in size and morphology. However, in contrast to WSPs, no impurities such as inorganic salts are apparent. The zinc oxide nanoparticles (ZnO) have a heterogeneous shape and size, ranging from 10 nm to over 100 nm. ZnO particles also appear as agglomerates, which are smaller than those of the carbonaceous particles, rarely exceeding 1 µm in size. The agglomeration of all tested particles could further be observed in cell culture experiments, as particles sedimented readily and agglomerates were visible under the light microscope on the cell layer. Comparable findings have been reported before for resuspended particulate matter from wood combustion (Danielsen et al. 2011), CB14 (Diabaté et al. 2011; Saber et al. 2012) and ZnO (Karlsson et al. 2008).

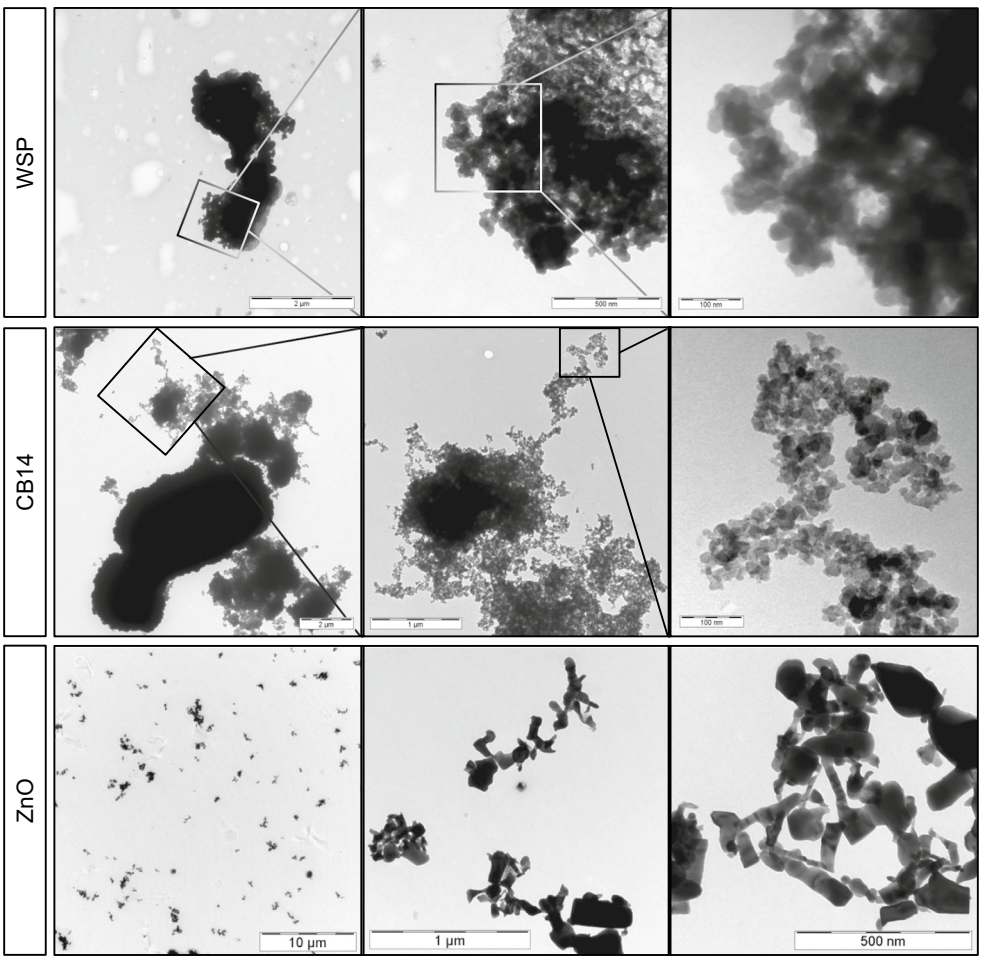

Fig. 1 Characterization of analysed particles. Transmission electron microscopic images of collected wood smoke particles (WSPs), carbon black nanoparticles (CB14) and zinc oxide nanoparticles (ZnO) at different magnifications

Table 1 Concentrations of selected PAHs in the WSP sample (RSD = relative standard deviation)

PAH	mg/kg	RSD (%)
Acenaphthene	<0.037	2
Acenaphthylene	2.59	2
Anthracene	6.3	5
Benz[a]anthracene	23.3	2
Benz[a]pyrene	18.6	2
Benzo[ghi]perylene	17	2
Chrysene	42.3	2
Dibenz[ah]anthracene	1.4	2
Fluoranthene	103	2
Fluorene	0.929	1
Indeno[1,2,3-cd]pyrene	11	2
Naphthalene	0.715	5
Phenanthrene	52.1	1
Pyrene	109	1
sum Benzo[b,k]fluoranthene	52.2	3
Sum of all analysed PAHs	948.0	
B[a]P Toxic equivalent value Nisbet and LaGoy (1992)	35.2	

The chemical analysis of the WSP samples detected several PAHs in the WSP samples, with a total amount of 948 mg/kg. The values for selected PAHs (16 EPA priority PAHs) are shown in Table 1. The full list of analysed organic contaminants for all particle samples, including the internal standards used for quantification, is available in Supplementary Table S1. Additional chemical analysis—quantification of total elementary carbon (EC), organic carbon (OC), inorganic salts (Gauggel et al. 2012) and metals (Gauggel-Lewandowski et al. 2013)—has been published previously and is summarized in Supplementary Table S2. The WSPs are derived from a fuel consisting of wood briquettes, split logs comprised of hard and soft wood, as well as waste wood, the latter being presumably responsible for the relatively high Fe content in the particle samples (Gauggel et al. 2012; Gauggel-Lewandowski et al. 2013). The other analysed parameters are within the expected range for typical wood combustions (Schmidl et al. 2008; Orasche et al. 2012, 2013; Torvela et al. 2014a) and vary with the experimental conditions, such as fuel type, stove type and operation. The CB14 and ZnO nanoparticles are specified by the manufacturer as >99 % pure carbon and ZnO, respectively. Although CB14 nanoparticles have previously been found to also contain low but non-negligible amounts of PAHs with biological impact in vivo (Borm et al. 2005), our chemical analysis of the CB14 did not detect the presence of biologically relevant PAHs. The ZnO nanoparticles were found to contain high amounts of fatty acids, presumably used as dispersant (Suppl. Table S1).

Cytotoxicity of particles

The acute toxicity of WSPs was determined by measuring the mitochondrial activity with the AlamarBlue® assay, as well as the membrane permeability by analysing the release of LDH into the medium. After 24 h incubation, the A549 cells neither show a reduction in the mitochondrial activity nor an elevated LDH secretion at all tested concentrations (Fig. 2a, b). Similarly, CB14 did not reduce, but rather slightly increase metabolic activity, and neither induced LDH release over the entire concentration range (Fig. 2c, d). On the contrary, high levels of ZnO particles triggered toxicity (Fig. 2e, f) as also published previously (Deschamps et al. 2013). CdO was used as a positive control for the AlamarBlue® assay because it reduces mitochondrial activity, while it does not impair cell membrane integrity at the tested concentrations (Fig. S1).

Inflammatory responses after exposure to WSPs

Secretion of the pro-inflammatory cytokine IL-8 into the supernatant was measured after 24 h incubation with WSPs by an ELISA assay. CdO particles were used as a positive control. No elevated secretion of IL-8 could be observed for the WSP-treated cells. Instead, the highest tested WSP concentration led to a significant decrease in detectable IL-8 (Fig. 3a). To test whether the observed reduction in detected IL-8 might be due to adsorption of the protein on the WSP surface, we incubated recombinant IL-8 with increasing concentrations of WSPs in serum-free medium and analysed the IL-8 remaining in the supernatant after 24 h. Indeed, IL-8 recovery diminished significantly with increasing WSP concentrations (Fig. S2). IL-8 mRNA levels, measured by qPCR, support the negative results from the ELISA. No significant change in IL-8 expression was observed after both 4 and 24 h, except a slight increase for the highest concentration at 24 h (Fig. 3b).

Cellular ROS formation after treatment with particles

We investigated the potency of WSPs to induce ROS formation by oxidation of the fluorogenic probe dihydrodichlorofluorescein (H_2DCF) to fluorescent DCF in A549 cells. After 3 h incubation, the WSPs led to a significant increase in H_2DCF oxidation in a dose-dependent manner (Fig. 4a). In addition, CB14 and ZnO NPs also induced the formation of ROS in A549 cells 3 h after exposure (Fig. 4b, c). However, the magnitude of H_2DCF oxidation differed considerably between these substances: the cellular ROS formation after treatment of cells with WSP and ZnO particles was comparable, but much lower than in cells exposed to CB14.

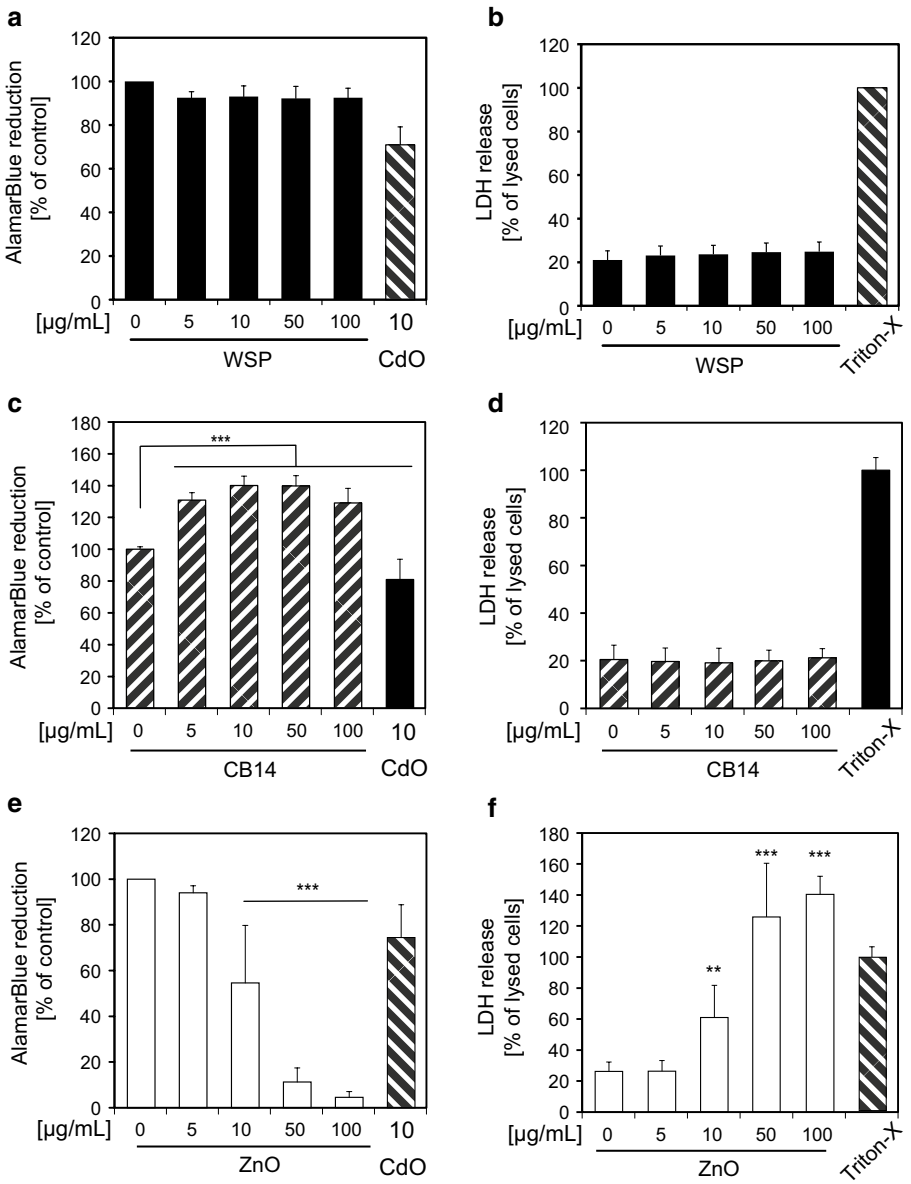

Fig. 2 Effects of particle treatment on viability and membrane integrity of A549 cells. Cells are treated with collected WSPs (**a**, **b**), CB14 (**c**, **d**) and ZnO NP (**e**, **f**) at 5, 10, 50 and 100 µg/mL or with CdO at 10 µg/mL in medium without FCS or in particle-free medium for 24 h. Cell viability is analysed using AlamarBlue® reagent (**a**, **c**, **e**) and is reported relative to negative controls (100 %). Membrane integrity is detected by LDH release (**b**, **d**, **f**) and is reported relative to positive controls (cells completely lysed with 1 % (WSP) or 0.1 % (CB14, ZnO) Triton X-100). Results are the means + SD of six independent experiments with three replicates each (WSP) and the means + SD of nine samples from three independent experiments (CB14) or six samples from two independent experiments (ZnO). (*$p < 0.05$, **$p < 0.01$, ***$p < 0.001$ compared to controls)

Interestingly, when H_2DCF oxidation is normalized to the EC concentration of the tested WSP suspensions, WSPs and CB14 show similar efficiencies (Fig. 4d). This suggests that EC is one of the main parameters driving ROS formation by WSPs. To further elucidate the impact of metals on ROS formation by WSPs, we reduced the bioavailability of metal ions using the transition metal chelator DFO, which has a high stability constant for Fe^{3+} but also chelates Zn^{2+} and other metal ions with lower specificity. Whereas DFO alone had no effect on ROS status in cells treated with particle-free medium or on CB14-induced ROS formation, it completely abrogated ZnO-mediated H_2DCF oxidation (Fig. 4e). Of note, enhanced ROS levels in response to WSPs were partially reduced by DFO. Hence, although the soot component of WSPs plays a major role in ROS formation, the metals in addition contribute significantly.

Regulation of heme oxygenase 1 by WSPs

Cells might react to oxidative challenges with an anti-oxidative response. One well-documented anti-oxidative key enzyme is heme oxygenase 1 (HO-1). HO-1 counteracts oxidative stress by catalysing the first and rate-limiting step in oxidative heme degradation, which additionally produces the anti-oxidative biliverdin (Choi and Alam 1996). We studied the regulation of HO-1 after exposure to WSPs in order to assess the cellular response following the perturbation of the redox equilibrium as indicated by the DCF assay. In contrast to expectations, even high WSP

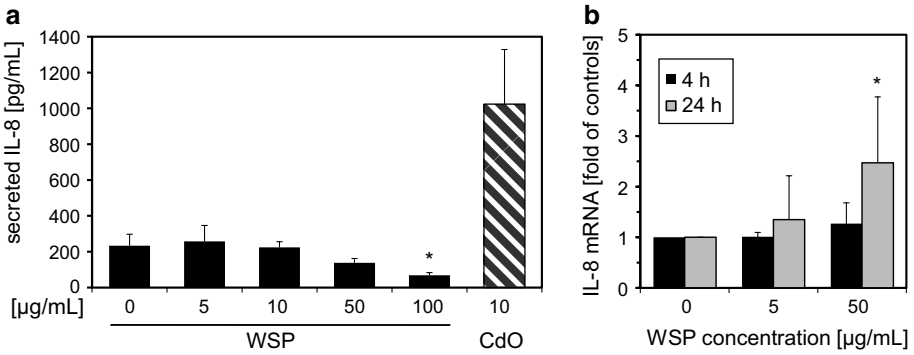

Fig. 3 WSPs do not increase the secretion of the pro-inflammatory cytokine IL-8 but increase the expression of IL-8 mRNA slightly. Cells are treated with collected WSPs at 5, 10, 50 and 100 µg/mL or with CdO at 10 µg/mL in medium without FCS or particle-free medium for 24 h. IL-8 secreted into the supernatant is measured by ELISA (**a**). CdO served as a positive control. Results are the means + SD of nine samples originating from three independent experiments. (*=$p < 0.05$ compared to control). IL-8 mRNA is determined by qRT-PCR after 4 and 24 h (**b**). Results are the means + SD of 4 samples originating from two independent experiments

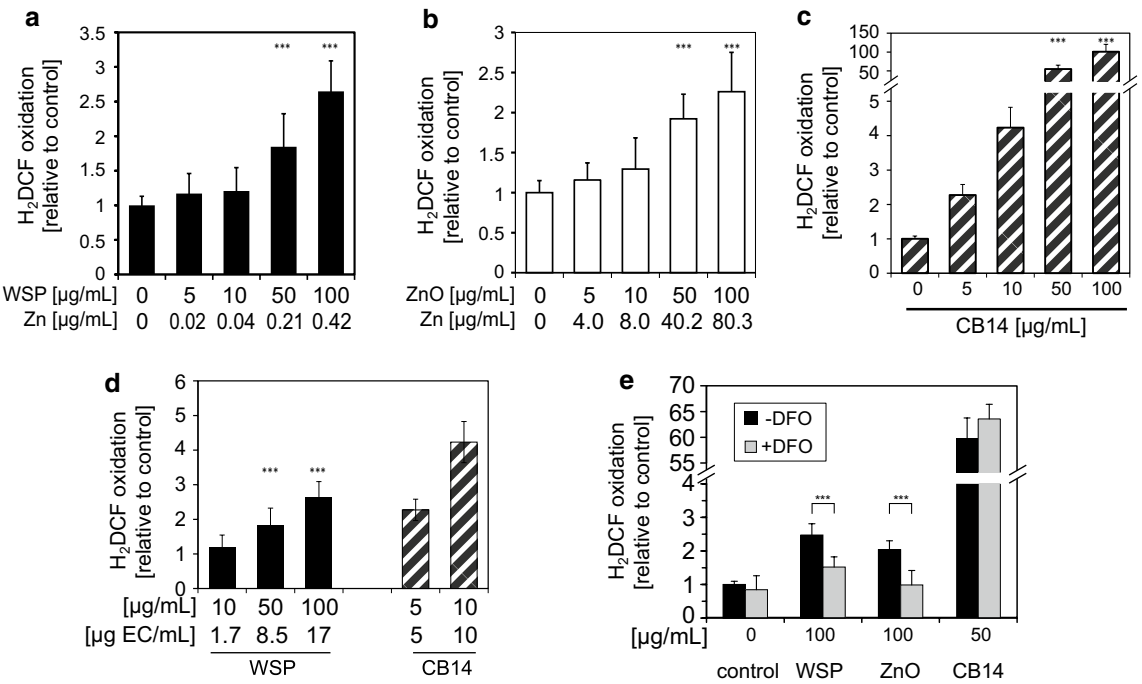

Fig. 4 WSPs induce intracellular reactive oxygen species (ROS), mainly caused by elemental carbon and metallic constituents. A549 cells are treated with different concentrations of wood smoke particles (**a**, **d**), zinc oxide nanoparticles (**b**) and carbon black nanoparticles (**c**, **d**) in medium without FCS or particle-free medium for 3 h. Additionally, particle-treated cells are co-treated with the transition metal chelator DFO to reduce the metal-mediated ROS formation (**e**). ROS formation is monitored by measuring H_2DCF oxidation, and values are expressed relative to particle-free controls. In **a**, **b**, the relative amount of Zn content is calculated for better comparison of WSPs and ZnO particles. Similarly, in **d** the relative content of elemental carbon (EC) for the different concentrations of WSPs and CB particles is depicted. Results are the mean + SD of at least nine (**a**, **e**) or six (**b**, **c**, **d**) samples originating from at least three (**a**) or two (**b**–**e**) independent experiments, ***$p < 0.001$ compared to the corresponding control. One-sided Welch's t tests are used in (**e**) to test for reduced H_2DCF oxidation by DFO co-treatment

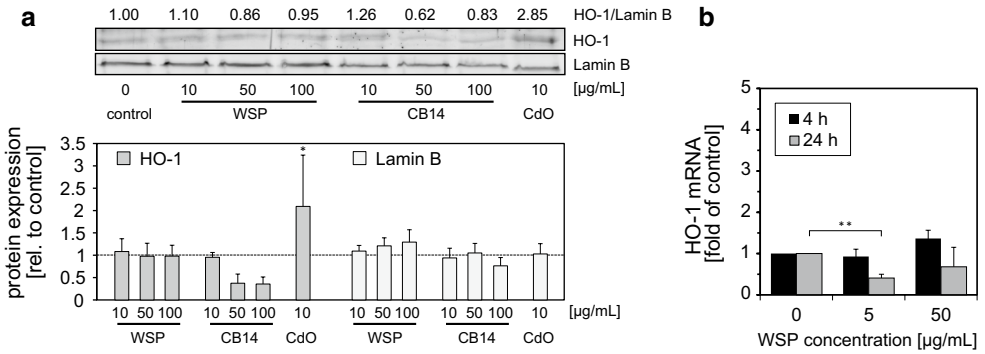

Fig. 5 In spite of intracellular ROS formation, WSPs and CB14 do not induce anti-oxidative HO-1. A549 cells are treated with 0, 10, 50 or 100 µg/mL of WSPs or CB14 in medium without FCS. CdO is used as a positive control. After 24 h, HO-1 protein levels are determined from whole cell lysates by immunoblotting (**a**). Lamin B served as the loading control. Shown is one representative blot and the respective normalized HO-1/Lamin B ratio (*top*) as well as the quantification of HO-1 and Lamin B levels (*bottom*), normalized to control + SD based on four blots from two independent experiments. HO-1 mRNA is determined by qRT-PCR (**b**). Results shown are the mean + SD of four samples originating from two independent experiments (*$p < 0.05$ compared as indicated)

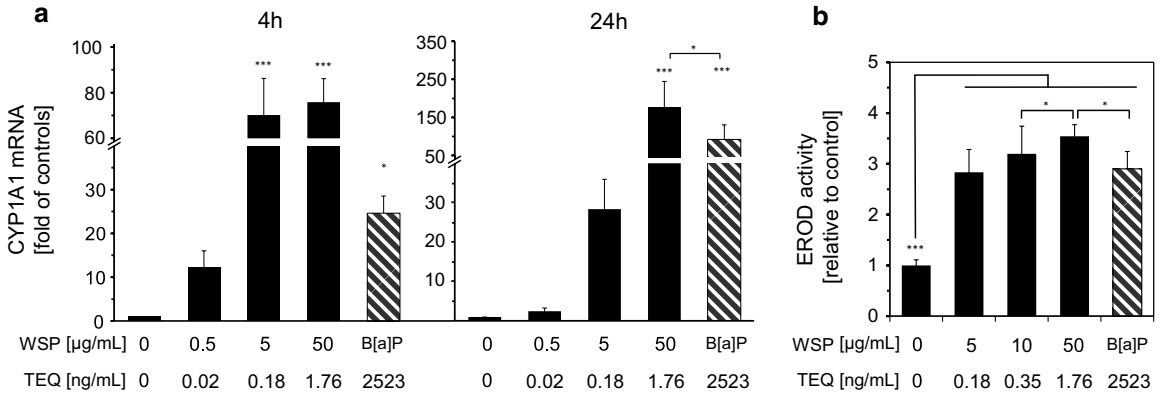

Fig. 6 PAHs bound to WSP particles induce a stronger CYP1A1 expression and EROD activity than a dissolved model PAH. A549 cells are treated with collected WSPs at the indicated concentrations or 10 µM of the model PAH B[a]P suspended in serum-free medium. CYP1A1 mRNA levels are measured by qPCR after 4 h and 24 h (**a**). CYP1A1 enzyme activity is measured with the EROD assay 48 h after treatment (**b**). For a better comparison, toxicity equivalents (TEQ) are calculated as indicated for the different concentrations of WSPs and the B[a]P suspension. Results are the mean + SD of four (qPCR) or six (EROD) samples originating from two independent experiments. Post hoc Tukey HSD is used for multiple comparisons of treatments (*$p < 0.05$, ***$p < 0.001$ compared to control except if otherwise indicated)

concentrations failed to induce the expression of HO-1 at the mRNA and protein level (Fig. 5a, b). Even treatment with CB14, which more strongly promoted H_2DCF oxidation, did not lead to a detectable increase in the HO-1 protein.

Induction of cytochrome P450 1A1 (CYP1A1) by PAHs bound to WSPs

CYP1A1 expression was strongly increased after 4 and 24 h treatment with WSPs (Fig. 6a, b). After 4 h, a concentration as little as 5 µg/mL led to a 70-fold increase in CYP1A1 expression, compared to the control. At this time point, a higher concentration was not able to induce a stronger effect. In contrast, after 24 h exposure, the WSPs induced CYP1A1 expression with a slightly different pattern. Here, a dose-dependent induction was observed over the whole range of the tested concentrations. Notably, after 24 h the magnitude of CYP1A1 mRNA increase was lower than after 4 h for low concentrations (0.5 µg/mL and 5 µg/mL), while expression increased with a 24-h exposure of 50 µg/mL as well as the much higher concentrated positive control B[a]P.

In line with the results from the qPCR, WSPs also increased the cytochrome P450-associated enzymatic activity, as was measured by the EROD (ethoxyresorufin-O-deethylase) assay (Fig. 6b). The fluorogenic 7-ER is cytochrome P450 dependently deethylated to form the

fluorescent product resorufin, which can then easily be quantified (Eichbaum et al. 2014). EROD activity values showed a dose-dependent increase after 48 h of treatment with WSPs, which were even slightly more potent in enhancing enzymatic activity compared to B[a]P.

Discussion

WSPs do not trigger acute cytotoxicity nor induce pro-inflammatory IL-8

In this study, the investigated WSPs did not induce signs of acute toxicity (Fig. 2). This finding is in line with the majority of other in vitro studies with WSPs using epithelial cells (Kocbach Bølling et al. 2009; Danielsen et al. 2011); however, for high particle concentrations, acute toxicity has been reported in murine macrophages (Jalava et al. 2010; Tapanainen et al. 2011).

Furthermore, WSPs did not lead to elevated expression and secretion of the pro-inflammatory cytokine IL-8. Instead, the highest tested WSP concentration significantly decreased detectable IL-8 (Fig. 3a). Even when not challenged, A549 cells secrete IL-8 in small amounts. Given the high specific surface area of the tested particles, adsorption of cytokines to the surface could be an explanation for the decrease in detectable IL-8. Indeed, this could be confirmed experimentally (Fig. S2). Such interference with ELISA assays has also been observed before for WSPs and other particles (Herseth et al. 2013). However, besides confirming previous findings (Danielsen et al. 2011), there are also studies that document expression and secretion of inflammatory proteins after challenge of cultured cells with WSPs (Kocbach Bølling et al. 2009; Corsini et al. 2013). The divergent results are most likely explained by differences in the individual composition and size of the tested WSPs, as well as the cell culture models employed. In fact, it has been observed that different PAH and metal compositions of diesel exhaust particles lead to qualitative differences in the inflammatory response (Totlandsdal et al. 2015). Furthermore, monocytes in mono and co-culture with epithelial lung cells seem to be more sensitive, indicated by the enhanced release of inflammatory markers (Kocbach et al. 2008a, b). Some inhalation studies with human volunteers found limited evidence for mild airway inflammation (Riddervold et al. 2012; Ghio et al. 2012), whereas others reported no alterations in markers of systemic inflammation (Sehlstedt et al. 2010; Forchhammer et al. 2012; Stockfelt et al. 2012; Jensen et al. 2014). Thus, the relevance of an acute inflammatory response observed in vitro needs to be explored in an entire organism such as rodents or human volunteers.

WSPs induce ROS formation but do not trigger further anti-oxidative responses in A549 cells

One of the central paradigms of particle toxicology is the formation of reactive oxygen species (ROS) leading to adverse health effects (Nel et al. 2006). Treatment of A549 cells with WSPs led to a significant increase in H_2DCF oxidation in a dose-dependent manner (Fig. 4a). WSPs contain two major constituents, which could be causative for particle-mediated ROS formation: soot and metal compounds. Soot primarily consists of elementary carbon with a high specific surface area, while transition metals can lead to elevated formation of ROS, e.g. by Fenton-like reactions or inhibition of anti-oxidative processes (Oberdörster et al. 2005; Nel et al. 2006; Limbach et al. 2007). We therefore chose carbon black (CB14) as well as ZnO nanoparticles to mimic the soot and Zn fraction of WSPs, respectively (Torvela et al. 2014a), and tested them separately for their potency to mediate ROS formation. CB14 induces intracellular ROS formation even at low doses, while no toxicity could be observed over the whole tested concentration range, similarly to WSPs (Fig. 2). It is interesting to note that CB14 exposure even leads to an increased reduction in AlamarBlue reagent, which might be due to the catalytic activity of the CB14 surface, facilitating the intra- or extracellular reduction of the dye (Oh et al. 2012). Interestingly, when H_2DCF oxidation is normalized to the EC concentration of the tested WSP suspensions, WSPs and CB14 show similar efficiencies (Fig. 4). This suggests that EC is one of the main parameters driving ROS formation by WSPs. A correlation of higher H_2DCF oxidation with increasing surface area of soot-like particles has been reported before (Chuang et al. 2011). The WSPs tested in our study provoked a comparable, but slightly weaker level of ROS formation than CB14 when the EC content is used as dose metric. Possibly, organics and inorganics covering the surface of WSPs diminish the available surface area and thus the activity. Cellular ROS formation after treatment with ZnO nanoparticles was much lower than for CB14 (Fig. 4). Moreover, enhanced ROS formation was only observed at high ZnO concentrations, which are well beyond the levels of Zn present in the tested WSP samples, indicating that Zn is unlikely to contribute to H_2DCF oxidation in response to WSPs. Interestingly, efficient combustion conditions, although reducing overall emissions, lead to enrichment of Zn in the emitted particle mass. It has recently indeed been shown that Zn-rich WSPs sampled from an efficient combustion source increased ROS formation and toxicity in murine macrophages and inflammation in murine lungs, while particles derived from less efficient combustion did not (Happo et al. 2013; Uski et al. 2014).

The ratio of Fe and Zn in wood smoke particles (WSPs) is quite variable, dependent primarily on the source of

wood and combustion conditions. The Fe content of the tested particles in the present study is relatively high, whereas the amount of Zn is within the range found in most other studies. Combustion of hardwoods usually results in particle emissions with roughly equal Fe and Zn concentrations, and combustion of other wood fuels, however, can also generate particles with 5–20 times more Zn than Fe (Schmidl et al. 2008; Orasche et al. 2012; Gauggel-Lewandowski et al. 2013). ZnO nanoparticles thus were chosen as a model for metal constituents as Zn is on average the dominating metal species in particles derived from wood combustion (Schmidl et al. 2008; Orasche et al. 2012; Gauggel-Lewandowski et al. 2013) and is suspected to be of relevance for adverse effects promoted by wood smoke particles (Torvela et al. 2014b). Yet, our results suggest that the Zn content in the tested wood smoke particles is too low to lead to the observed ROS formation, in line with our previous studies (Deschamps et al. 2013) where enhanced ROS formation was observed only at high ZnO concentrations. Unlike other transition metals such as Fe, Zn does not directly promote generation of ROS. Rather the indirect action on redox sensing thiol groups in, for example, anti-oxidative enzymes or by impairing mitochondrial respiration is of relevance in this context (Wu et al. 2013).

In our study, the Fe content of the WSPs (~12 µg Fe/mL) seems to be important, as the iron chelator DFO decreased ROS production (Fig. 4). Interestingly, we previously studied the impact of two differently sized iron oxide nanoparticles on ROS formation using the same cell line and assay protocol but found no increasing ROS levels at concentrations of ~140 µg Fe/mL (Panas et al. 2013). However, for Fe-containing fly ash particles (~1.7–3.4 µg Fe/mL), we also observed ROS formation in macrophages which could be completely suppressed by co-incubation with the iron chelator DFO (Fritsch-Decker et al. 2011). It is possible that Fe localized in combustion-derived particles has a higher bioavailability because the particles act as carriers for endocytosis and lead to liberation of Fe in the lysosome.

The absence of an anti-oxidative response as evidenced by a lack of HO-1 induction (Fig. 5) despite ROS formation following WSP treatment has been noted before in A549 cells (Danielsen et al. 2011). However, the effect was cell type specific as the monocytic cell line THP-1 showed an increased HO-1 expression. Like in many lung cancer-derived cell lines, in A549 cells the regulatory KEAP1 protein is mutated, which leads to a persistent increase in the activation of the transcription factor NRF2 and subsequent up-regulation of anti-oxidative genes, e.g. HO-1 (Singh et al. 2006). Nevertheless, CdO particles, which served as a positive control in this study, and combustion-derived particles from other sources (Fukano et al. 2006) enhance expression of HO-1 in A549 cells. Yet, a higher baseline level of anti-oxidative gene expression may lead to a lower susceptibility towards oxidative damage in A549 cells. Therefore, a moderate increase in ROS levels by WSPs, as observed here, might not be sufficient to initiate an anti-oxidative response. Also, CB14 failed to trigger HO-1 expression although ROS formation was even more pronounced. CB14 rather decreased the levels of HO-1. Whether CB14 specifically triggers inhibition of gene expression or protein stability, or rather artificially interferes with detection of some proteins due the strong adsorption of proteins to its surface (Ruh et al. 2012), needs to be further investigated.

In order to explore the consequences of WSP-mediated ROS formation in more detail, cells with an intact NRF2 pathway, such as the bronchial epithelial cell line BEAS-2B, would be of advantage. Nevertheless, treatment of BEAS-2B cells with CB14 did not alter the levels of HO-1 expression despite strong formation of ROS (Diabaté et al. 2011). Thus, an alternative explanation for the disconnection of ROS formation and HO-1 induction by CB14 and possibly WSPs could be the localization and chemical nature of ROS, which are therefore unable to activate the NRF2 pathway. The overall relevance of oxidative stress for adverse effects of WSPs needs to be further explored especially with regard to the impact of different combustion conditions as discussed above. As residential wood combustion in conventional stoves emits substantial amounts of PAHs, we finally assessed the role of PAHs associated with the WSPs in downstream toxicological events.

PAHs bound to WSPs induce cytochrome P450 1A1

The investigated WSPs contain a range of toxicologically relevant PAHs (Table 1). CYP1A1 (Cytochrome P450, family 1, subfamily A, polypeptide 1) is involved in metabolic activation of PAHs and is transcriptionally up-regulated in response to PAHs. Therefore, CYP1A1 expression levels are a specific readout for the bioavailability of particle bound PAHs and their receptor activating potency. One of the most toxic PAHs is benz[a]pyrene (B[a]P) which upon binding to the aryl hydrocarbon receptor (AhR) is metabolized and thereby detoxified. Yet, metabolism also generates highly reactive genotoxic intermediates which can also trigger cell death (Schreck et al. 2009; Donauer et al. 2012). Thus, we also used B[a]P in our experiments as proxy for PAH toxicity. The affinity to the AhR and the metabolism of various PAHs is different when compared to B[a]P. Therefore, the so-called B[a]P toxic equivalent (TEQ) value provides an estimate of the toxicity of PAH mixtures expressed as benz[a]pyrene equivalent concentration (Nisbet and LaGoy 1992). There was a striking difference in the cellular response between the soluble B[a]P and the particle bound PAH mixture (Fig. 6). When the TEQ concentration of the different WSP suspensions are compared to the TEQ concentration of the soluble B[a]P (Table S1), the PAHs bound to WSPs are by several

orders of magnitude more potent to induce CYP1A1 than B[a]P. As PAHs are adsorbed on the particle surface, particles might serve as a vehicle to deliver PAHs to the cell either due to particle sedimentation and/or increasing PAH uptake via a "trojan horse" mechanism, where particles act as carriers for OC (Janssen et al. 2012; Gebel et al. 2014). Hence, the difference in CYP1A1 induction might simply be explained by an increased cellular dose of PAHs promoted by WSPs, whereas most of the suspended B[a]P remains in the supernatant and only a fraction enters the cell.

As shown above (Fig. 2), WSPs increased ROS formation; however, the underlying mechanisms of this result are poorly understood. Interestingly, metabolism of PAHs by CYP1A1 could also produce ROS (Briedé et al. 2004). PAHs might be metabolized by aldo-keto reductases to generate ROS, as has been seen in A549 cells (Park et al. 2008). To our knowledge, data on the response of human cells to PAHs after exposure to WSPs are scarce. In rats, neither inhalation of wood smoke nor exposure of lung explants to extracts of WSPs induced CYP1A1 expression (Iba et al. 2006). However, in rat liver cells WSPs strongly increased the expression of an AhR-dependent luciferase gene similar to the potent AhR ligand B[a]P (Gauggel et al. 2012), yet the response of endogenous CYP1A1 was not analysed. Rats are more sensitive to AhR ligands when compared to humans due to a polymorphism in the coding sequence of AhR, which enhances ligand affinity (Moriguchi et al. 2003). Therefore, our findings of a pronounced activation of AhR, and consequently, CYP1A1 by WSPs in human lung cells is quite significant also with respect to risk assessment, bearing in mind the key role of this pathway in carcinogenesis (Nebert and Dalton 2006).

Conclusion

The present study demonstrates that WSPs from residential wood burning induce ROS as well as a strong cellular response typical for exposure to PAHs. PAHs adsorbed to WSPs even more potently induced expression of CYP1A1 than B[a]P applied in suspension. Clearly, more studies are needed to address the bioavailability of PAHs bound to WSPs and the mechanism of particle and PAH interactions. As metabolic activation of PAHs is critically linked to genotoxicity, mutagenesis and carcinogenesis, the effect of WSPs on these endpoints needs to be critically evaluated in the future. The soot fraction and metals were found to be the most important factors for ROS formation. A brief summary of the results is shown in Fig. 7. Soot and especially PAH content are important parameters for WSP toxicity. Both can be reduced by the use of more efficient furnaces. Yet, enhanced combustion technologies might increase the relative metal content per mass and thus shift the profile of toxicity. Therefore, also a reduction in emitted metal species would be desirable, e.g. by the use of particle precipitation techniques in the off-gas. In perspective, our present study warrants further investigations on the toxicity of WSPs. As the response of cells to particle deposition in classical submerged experiments and at the air–liquid interface (ALI) might differ (Paur et al. 2008; Panas et al. 2014) in the future, lung cells should also be exposed at the ALI and adverse effects induced by wood smoke particles, but also the gas phase, need to be investigated in more detail including systems biology approaches (Oeder et al. 2015).

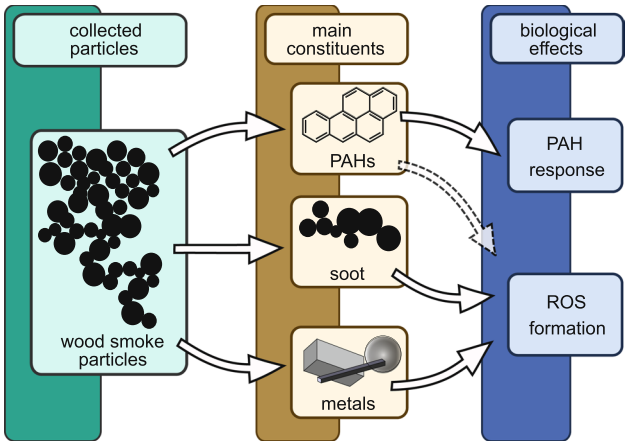

Fig. 7 Wood smoke particles (WSPs) derived from residential combustion are a complex mixture, containing toxic constituents, such as polycyclic aromatic hydrocarbons (PAHs), soot and metals. In human A549 lung cells, WSPs induce ROS formation as well as a strong PAH response. These effects can indeed be mimicked by individual substances representing the PAH and soot fraction of WSPs. B[a]P, representing one of the most potent PAHs, induced qualitatively the same PAH response (CYP1A1 gene expression, EROD activity). However, the WSP-bound PAHs are much more potent than pure B[a]P dissolved in medium. Treatment with carbon black nanoparticles, representing the carbonaceous soot fraction, led to a ROS formation comparable to treatment with WSPs when the elemental carbon content of both particle types is used as a metric. The metal chelator DFO partially prevented ROS formation mediated by WSPs suggesting that in addition to elemental carbon metals are also responsible for WSP-induced ROS formation

Acknowledgments We thank Silvia Andraschko for assistance with TEM, Sonja Mülhopt for providing the WSP samples as well as Susanne Gauggel and Daniel Dietrich for providing additional information on particle characterization. We are also grateful to Sean C. Sapcariu for language proofreading. This study was performed partially in the framework of the Helmholtz Virtual Institute for Complex Molecular System in Environmental Health—Aerosols and Health (HICE, www.hice-vi.eu). Within the HICE Virtual Institute, combustion aerosol emissions are studied by comprehensive physical and chemical analysis of the aerosols and by monitoring the molecular biological effects of the emissions on cultured cells.

Compliance with ethical standards

Conflict of interest The authors declare no conflicts of interest.

References

Aam BB, Fonnum F (2007) Carbon black particles increase reactive oxygen species formation in rat alveolar macrophages in vitro. Arch Toxicol 81:441–446. doi:10.1007/s00204-006-0164-3

Baird WM, Hooven LA, Mahadevan B (2005) Carcinogenic polycyclic aromatic hydrocarbon-DNA adducts and mechanism of action. Environ Mol Mutagen 45:106–114. doi:10.1002/em.20095

Belis CA, Karagulian F, Larsen BR, Hopke PK (2013) Critical review and meta-analysis of ambient particulate matter source apportionment using receptor models in Europe. Atmos Environ 69:94–108. doi:10.1016/j.atmosenv.2012.11.009

Beyersmann D, Hartwig A (2008) Carcinogenic metal compounds: recent insight into molecular and cellular mechanisms. Arch Toxicol 82:493–512. doi:10.1007/s00204-008-0313-y

BImSchG (2014) Bundes-Immissionsschutzgesetz (BImSchG). Bundesministerium der Justiz und für Verbraucherschutz, Germany

Bølling AK, Totlandsdal AI, Sallsten G, Braun A, Westerholm R, Bergvall C, Boman J, Dahlman HJ, Sehlstedt M et al (2012) Wood smoke particles from different combustion phases induce similar pro-inflammatory effects in a co-culture of monocyte and pneumocyte cell lines. Part Fibre Toxicol 9:45. doi:10.1186/1743-8977-9-45

Bologa A, Paur H-R, Woletz K (2011) Development and study of an electrostatic precipitator for small scale wood combustion. Int J Plasma Environ Sci Technol 5:168–173

Bonjour S, Adair-Rohani H, Wolf J, Bruce NG, Mehta S, Prüss-Ustün A, Lahiff M, Rehfuess EA, Mishra V et al (2013) Solid fuel use for household cooking: country and regional estimates for 1980–2010. Environ Health Perspect 121:784–790. doi:10.1289/ehp.1205987

Bønløkke JH, Riddervold IS, Grønborg TK, Skogstrand K, Hougaard DM, Barregard L, Sigsgaard T (2014) Systemic effects of wood smoke in a short-term experimental exposure study of atopic volunteers. J Occup Environ Med 56:177–183. doi:10.1097/JOM.0000000000000067

Borm PJA, Cakmak G, Jermann E, Weishaupt C, Kempers P, van Schooten FJ, Oberdörster G, Schins RPF (2005) Formation of PAH-DNA adducts after in vivo and vitro exposure of rats and lung cells to different commercial carbon blacks. Toxicol Appl Pharmacol 205:157–167. doi:10.1016/j.taap.2004.10.020

Briedé JJ, Godschalk RWL, Emans MTG, De Kok TMCM, Van Agen E, Van Maanen J, Van Schooten F-J, Kleinjans JCS (2004) In vitro and in vivo studies on oxygen free radical and DNA adduct formation in rat lung and liver during benzo[a]pyrene metabolism. Free Radic Res 38:995–1002. doi:10.1080/10715760400000976

Cassee FR, Héroux M-E, Gerlofs-Nijland ME, Kelly FJ (2013) Particulate matter beyond mass: recent health evidence on the role of fractions, chemical constituents and sources of emission. Inhal Toxicol 25:802–812. doi:10.3109/08958378.2013.850127

Choi AM, Alam J (1996) Heme oxygenase-1: function, regulation, and implication of a novel stress-inducible protein in oxidant-induced lung injury. Am J Respir Cell Mol Biol 15:9–19. doi:10.1165/ajrcmb.15.1.8679227

Chuang H-C, Jones TP, Lung S-CC, BéruBé KA (2011) Soot-driven reactive oxygen species formation from incense burning. Sci Total Environ 409:4781–4787. doi:10.1016/j.scitotenv.2011.07.041

Corsini E, Budello S, Marabini L, Galbiati V, Piazzalunga A, Barbieri P, Cozzutto S, Marinovich M, Pitea D et al (2013) Comparison of wood smoke PM2.5 obtained from the combustion of FIR and beech pellets on inflammation and DNA damage in A549 and THP-1 human cell lines. Arch Toxicol. doi: 10.1007/s00204-013-1071-z

Danielsen PH, Møller P, Jensen KA, Sharma AK, Wallin H, Bossi R, Autrup H, Mølhave L, Ravanat J-L et al (2011) Oxidative stress, DNA damage, and inflammation induced by ambient air and wood smoke particulate matter in human A549 and THP-1 cell lines. Chem Res Toxicol 24:168–184

Deschamps E, Weidler PG, Friedrich F, Weiss C, Diabaté S (2013) Characterization of indoor dust from Brazil and evaluation of the cytotoxicity in A549 lung cells. Environ Geochem Health. doi:10.1007/s10653-013-9560-9

Diabaté S, Bergfeldt B, Plaumann D, Uebel C, Weiss C (2011) Antioxidative and inflammatory responses induced by fly ash particles and carbon black in lung epithelial cells. Anal Bioanal Chem 401:3197–3212. doi:10.1007/s00216-011-5102-4

Dockery DW, Pope CA (1994) Acute respiratory effects of particulate air pollution. Annu Rev Public Health 15:107–132. doi:10.1146/annurev.pu.15.050194.000543

Donauer J, Schreck I, Liebel U, Weiss C (2012) Role and interaction of p53, BAX and the stress-activated protein kinases p38 and JNK in benzo(a)pyrene-diolepoxide induced apoptosis in human colon carcinoma cells. Arch Toxicol 86:329–337. doi:10.1007/s00204-011-0757-3

Eichbaum K, Brinkmann M, Buchinger S, Reifferscheid G, Hecker M, Giesy JP, Engwall M, van Bavel B, Hollert H (2014) In vitro bioassays for detecting dioxin-like activity—application potentials and limits of detection, a review. Sci Total Environ 487:37–48. doi:10.1016/j.scitotenv.2014.03.057

Ezzati M, Saleh H, Kammen DM (2000) The contributions of emissions and spatial microenvironments to exposure to indoor air pollution from biomass combustion in Kenya. Environ Health Perspect 108:833–839. doi:10.1289/ehp.00108833

Forchhammer L, Møller P, Riddervold IS, Bønløkke J, Massling A, Sigsgaard T, Loft S (2012) Controlled human wood smoke exposure: oxidative stress, inflammation and microvascular function. Part Fibre Toxicol 9:7. doi:10.1186/1743-8977-9-7

Fritsch-Decker S, Both T, Mülhopt S, Paur H, Weiss C, Diabaté S (2011) Regulation of the arachidonic acid mobilization in macrophages by combustion-derived particles. Part Fibre Toxicol 8:23. doi:10.1186/1743-8977-8-23

Fukano Y, Yoshimura H, Yoshida T (2006) Heme oxygenase-1 gene expression in human alveolar epithelial cells (A549) following exposure to whole cigarette smoke on a direct in vitro exposure system. Exp Toxicol Pathol 57:411–418. doi:10.1016/j.etp.2005.12.001

Garza KM, Soto KF, Murr LE (2008) Cytotoxicity and reactive oxygen species generation from aggregated carbon and carbonaceous nanoparticulate materials. Int J Nanomedicine 3:83–94

Gauggel S, Derreza-Greeven C, Wimmer J, Wingfield M, van der Burg B, Dietrich DR (2012) Characterization of biologically available wood combustion particles in cell culture medium. ALTEX 29:183–200

Gauggel-Lewandowski S, Heussner AH, Steinberg P, Pieterse B, van der Burg B, Dietrich DR (2013) Bioavailability and potential carcinogenicity of polycyclic aromatic hydrocarbons from wood combustion particulate matter in vitro. Chem Biol Interact. doi:10.1016/j.cbi.2013.05.015

Gebel T, Foth H, Damm G, Freyberger A, Kramer P-J, Lilienblum W, Röhl C, Schupp T, Weiss C et al (2014) Manufactured nanomaterials: categorization and approaches to hazard assessment. Arch Toxicol 88:2191–2211. doi:10.1007/s00204-014-1383-7

Ghio AJ, Soukup JM, Case M, Dailey LA, Richards J, Berntsen J, Devlin RB, Stone S, Rappold A (2012) Exposure to wood smoke particles produces inflammation in healthy volunteers. Occup Environ Med 69:170–175. doi:10.1136/oem.2011.065276

Greven FE, Krop EJ, Spithoven JJ, Burger N, Rooyackers JM, Kerstjens HA, van der Heide S, Heederik DJ (2012) Acute

respiratory effects in firefighters. Am J Ind Med 55:54–62. doi:10.1002/ajim.21012

Happo MS, Uski O, Jalava PI, Kelz J, Brunner T, Hakulinen P, Mäki-Paakkanen J, Kosma V-M, Jokiniemi J et al (2013) Pulmonary inflammation and tissue damage in the mouse lung after exposure to PM samples from biomass heating appliances of old and modern technologies. Sci Total Environ 443:256–266. doi:10.1016/j.scitotenv.2012.11.004

Herseth JI, Totlandsdal AI, Bytingsvik S, Kaur J, Noer M, Bølling AK (2013) The challenge of obtaining correct data for cellular release of inflammatory mediators after in vitro exposure to particulate matter. Toxicol Lett 221:110–117. doi:10.1016/j.toxlet.2013.06.209

Iba MM, Fung J, Chung L, Zhao J, Winnik B, Buckley BT, Chen LC, Zelikoff JT, Kou YR (2006) Differential inducibility of rat pulmonary CYP1A1 by cigarette smoke and wood smoke. Mutat Res 606:1–11. doi:10.1016/j.mrgentox.2006.02.007

Jalava PI, Salonen RO, Nuutinen K, Pennanen AS, Happo MS, Tissari J, Frey A, Hillamo R, Jokiniemi J et al (2010) Effect of combustion condition on cytotoxic and inflammatory activity of residential wood combustion particles. Atmos Environ 44:1691–1698. doi:10.1016/j.atmosenv.2009.12.034

Janssen NA, Gerlofs-Nijland ME, Lanki T, Salonen RO, Cassee F, Hoek G, Fischer P, Brunekreef B, Krzyzanowski M (2012) Health effects of black carbon. WHO Regional Office for Europe, Copenhagen, pp 1–86

Jensen A, Karottki DG, Christensen JM, Bønløkke JH, Sigsgaard T, Glasius M, Loft S, Møller P (2014) Biomarkers of oxidative stress and inflammation after wood smoke exposure in a reconstructed Viking Age house. Environ Mol Mutagen 55:652–661. doi:10.1002/em.21877

Johansson LS, Leckner B, Gustavsson L, Cooper D, Tullin C, Potter A (2004) Emission characteristics of modern and old-type residential boilers fired with wood logs and wood pellets. Atmos Environ 38:4183–4195. doi:10.1016/j.atmosenv.2004.04.020

Johnston FH, Henderson SB, Chen Y, Randerson JT, Marlier M, Defries RS, Kinney P, Bowman DMJS, Brauer M (2012) Estimated global mortality attributable to smoke from landscape fires. Environ Health Perspect 120:695–701. doi:10.1289/ehp.1104422

Karlsson HL, Cronholm P, Gustafsson J, Möller L (2008) Copper oxide nanoparticles are highly toxic: a comparison between metal oxide nanoparticles and carbon nanotubes. Chem Res Toxicol 21:1726–1732. doi:10.1021/tx800064j

Kato M, Loomis D, Brooks LM, Gattas GFJ, Gomes L, Carvalho AB, Rego MAV, DeMarini DM (2004) Urinary biomarkers in charcoal workers exposed to wood smoke in Bahia State, Brazil. Cancer Epidemiol Biomarkers Prev 13:1005–1012

Kocbach Bølling A, Pagels J, Yttri KE, Barregard L, Sallsten G, Schwarze PE, Boman C (2009) Health effects of residential wood smoke particles: the importance of combustion conditions and physicochemical particle properties. Part Fibre Toxicol 6:29. doi:10.1186/1743-8977-6-29

Kocbach A, Herseth JI, Låg M, Refsnes M, Schwarze PE (2008a) Particles from wood smoke and traffic induce differential pro-inflammatory response patterns in co-cultures. Toxicol Appl Pharmacol 232:317–326. doi:10.1016/j.taap.2008.07.002

Kocbach A, Namork E, Schwarze PE (2008b) Pro-inflammatory potential of wood smoke and traffic-derived particles in a monocytic cell line. Toxicology 247:123–132. doi:10.1016/j.tox.2008.02.014

Limbach LK, Wick P, Manser P, Grass RN, Bruinink A, Stark WJ (2007) Exposure of engineered nanoparticles to human lung epithelial cells: influence of chemical composition and catalytic activity on oxidative stress. Environ Sci Technol 41:4158–4163. doi:10.1021/es062629t

McCracken JP, Smith KR, Díaz A, Mittleman MA, Schwartz J (2007) Chimney stove intervention to reduce long-term wood smoke exposure lowers blood pressure among Guatemalan women. Environ Health Perspect 115:996–1001. doi:10.1289/ehp.9888

Monteiller C, Tran L, MacNee W, Faux S, Jones A, Miller B, Donaldson K (2007) The pro-inflammatory effects of low-toxicity low-solubility particles, nanoparticles and fine particles, on epithelial cells in vitro: the role of surface area. Occup Environ Med 64:609–615. doi:10.1136/oem.2005.024802

Moriguchi T, Motohashi H, Hosoya T, Nakajima O, Takahashi S, Ohsako S, Aoki Y, Nishimura N, Tohyama C et al (2003) Distinct response to dioxin in an arylhydrocarbon receptor (AHR)-humanized mouse. Proc Natl Acad Sci U S A 100:5652–5657. doi:10.1073/pnas.1037886100

Naeher LP, Brauer M, Lipsett M, Zelikoff JT, Simpson CD, Koenig JQ, Smith KR (2007) Woodsmoke health effects: a review. Inhal Toxicol 19:67–106. doi:10.1080/08958370600985875

Nebert DW, Dalton TP (2006) The role of cytochrome P450 enzymes in endogenous signalling pathways and environmental carcinogenesis. Nat Rev Cancer 6:947–960. doi:10.1038/nrc2015

Neitzel R, Naeher LP, Paulsen M, Dunn K, Stock A, Simpson CD (2009) Biological monitoring of smoke exposure among wildland firefighters: a pilot study comparing urinary methoxyphenols with personal exposures to carbon monoxide, particular matter, and levoglucosan. J Expo Sci Environ Epidemiol 19:349–358. doi:10.1038/jes.2008.21

Nel A, Xia T, Mädler L, Li N (2006) Toxic potential of materials at the nanolevel. Science 311:622–627. doi:10.1126/science.1114397

Nisbet ICT, LaGoy PK (1992) Toxic equivalency factors (TEFs) for polycyclic aromatic hydrocarbons (PAHs). Regul Toxicol Pharmacol 16:290–300. doi:10.1016/0273-2300(92)90009-X

Noonan CW, Ward TJ, Navidi W, Sheppard L (2012) A rural community intervention targeting biomass combustion sources: effects on air quality and reporting of children's respiratory outcomes. Occup Environ Med 69:354–360. doi:10.1136/oemed-2011-100394

O'Brien J, Wilson I, Orton T, Pognan F (2000) Investigation of the Alamar Blue (resazurin) fluorescent dye for the assessment of mammalian cell cytotoxicity. Eur J Biochem 267:5421–5426

Oberdörster G, Maynard A, Donaldson K, Castranova V, Fitzpatrick J, Ausman K, Carter J, Karn B, Kreyling W et al (2005) Principles for characterizing the potential human health effects from exposure to nanomaterials: elements of a screening strategy. Part Fibre Toxicol 2:8. doi:10.1186/1743-8977-2-8

Oeder S, Kanashova T, Sippula O, Sapcariu SC, Streibel T, Arteaga-Salas JM, Passig J, Dilger M, Paur H-R et al (2015) Particulate matter from both heavy fuel oil and diesel fuel shipping emissions show strong biological effects on human lung cells at realistic and comparable in vitro exposure conditions. PLoS One 10:e0126536. doi:10.1371/journal.pone.0126536

Oh S-Y, Son J-G, Lim O-T, Chiu PC (2012) The role of black carbon as a catalyst for environmental redox transformation. Environ Geochem Health 34(Suppl 1):105–113. doi:10.1007/s10653-011-9416-0

Orasche J, Schnelle-Kreis J, Abbaszade G, Zimmermann R (2011) Technical note: in-situ derivatization thermal desorption GC-TOFMS for direct analysis of particle-bound non-polar and polar organic species. Atmos Chem Phys 11:8977–8993. doi:10.5194/acp-11-8977-2011

Orasche J, Seidel T, Hartmann H, Schnelle-Kreis J, Chow JC, Ruppert H, Zimmermann R (2012) Comparison of emissions from wood combustion. Part 1: Emission factors and characteristics from different small-scale residential heating appliances considering particulate matter and polycyclic aromatic hydrocarbon (PAH)-related toxicological potential of particle-bound organic species. Energy & Fuels 26:6695–6704. doi:10.1021/ef301295k

Orasche J, Schnelle-Kreis J, Schön C, Hartmann H, Ruppert H, Arteaga-Salas JM, Zimmermann R (2013) Comparison of

emissions from wood combustion. Part 2: impact of combustion conditions on emission factors and characteristics of particle-bound organic species and polycyclic aromatic hydrocarbon (PAH)-related toxicological potential. Energy & Fuels 27:1482–1491. doi:10.1021/ef301506h

Panas A, Marquardt C, Nalcaci O, Bockhorn H, Baumann W, Paur H-R, Mülhopt S, Diabaté S, Weiss C (2013) Screening of different metal oxide nanoparticles reveals selective toxicity and inflammatory potential of silica nanoparticles in lung epithelial cells and macrophages. Nanotoxicology 7:259–273. doi:10.3109/17435390.2011.652206

Panas A, Comouth A, Saathoff H, Leisner T, Al-Rawi M, Simon M, Seemann G, Dössel O, Mülhopt S et al (2014) Silica nanoparticles are less toxic to human lung cells when deposited at the air–liquid interface compared to conventional submerged exposure. Beilstein J Nanotechnol 5:1590–1602. doi:10.3762/bjnano.5.171

Park J-H, Mangal D, Tacka KA, Quinn AM, Harvey RG, Blair IA, Penning TM (2008) Evidence for the aldo-keto reductase pathway of polycyclic aromatic trans-dihydrodiol activation in human lung A549 cells. Proc Natl Acad Sci USA 105:6846–6851. doi:10.1073/pnas.0802776105

Paur H-R, Mülhopt S, Weiss C, Diabaté S (2008) In vitro exposure systems and bioassays for the assessment of toxicity of nanoparticles to the human lung. J Consum Prot food Saf 3:319–329

Pudasainee D, Paur HR, Fleck S, Seifert H (2014) Trace metals emission in syngas from biomass gasification. Fuel Process Technol 120:54–60. doi:10.1016/j.fuproc.2013.12.010

Pulskamp K, Diabaté S, Krug HF (2007) Carbon nanotubes show no sign of acute toxicity but induce intracellular reactive oxygen species in dependence on contaminants. Toxicol Lett 168:58–74. doi:10.1016/j.toxlet.2006.11.001

Riddervold IS, Bønløkke JH, Olin A-C, Grønborg TK, Schlünssen V, Skogstrand K, Hougaard D, Massling A, Sigsgaard T (2012) Effects of wood smoke particles from wood-burning stoves on the respiratory health of atopic humans. Part Fibre Toxicol 9:12. doi:10.1186/1743-8977-9-12

Ruh H, Kühl B, Brenner-Weiss G, Hopf C, Diabaté S, Weiss C (2012) Identification of serum proteins bound to industrial nanomaterials. Toxicol Lett 208:41–50. doi:10.1016/j.toxlet.2011.09.009

Saber AT, Jensen KA, Jacobsen NR, Birkedal R, Mikkelsen L, Møller P, Loft S, Wallin H, Vogel U (2012) Inflammatory and genotoxic effects of nanoparticles designed for inclusion in paints and lacquers. Nanotoxicology 6:453–471. doi:10.3109/17435390.2011.587900

Sanhueza PA, Torreblanca MA, Diaz-Robles LA, Schiappacasse LN, Silva MP, Astete TD (2009) Particulate Air pollution and health effects for cardiovascular and respiratory causes in Temuco, Chile: a wood-smoke-polluted urban area. J Air Waste Manage Assoc 59:1481–1488. doi:10.3155/1047-3289.59.12.1481

Schmidl C, Marr IL, Caseiro A, Kotianová P, Berner A, Bauer H, Kasper-Giebl A, Puxbaum H (2008) Chemical characterisation of fine particle emissions from wood stove combustion of common woods growing in mid-European Alpine regions. Atmos Environ 42:126–141. doi:10.1016/j.atmosenv.2007.09.028

Schmittgen TD, Livak KJ (2008) Analyzing real-time PCR data by the comparative CT method. Nat Protoc 3:1101–1108. doi:10.1038/nprot.2008.73

Schreck I, Chudziak D, Schneider S, Seidel A, Platt KL, Oesch F, Weiss C (2009) Influence of aryl hydrocarbon- (Ah) receptor and genotoxins on DNA repair gene expression and cell survival of mouse hepatoma cells. Toxicology 259:91–96. doi:10.1016/j.tox.2009.02.006

Sehlstedt M, Dove R, Boman C, Pagels J, Swietlicki E, Löndahl J, Westerholm R, Bosson J, Barath S et al (2010) Antioxidant airway responses following experimental exposure to wood smoke in man. Part Fibre Toxicol 7:21. doi:10.1186/1743-8977-7-21

Singh A, Misra V, Thimmulappa RK, Lee H, Ames S, Hoque MO, Herman JG, Baylin SB, Sidransky D et al (2006) Dysfunctional KEAP1-NRF2 interaction in non-small-cell lung cancer. PLoS Med 3:e420. doi:10.1371/journal.pmed.0030420

Stockfelt L, Sallsten G, Olin A-C, Almerud P, Samuelsson L, Johannesson S, Molnar P, Strandberg B, Almstrand A-C et al (2012) Effects on airways of short-term exposure to two kinds of wood smoke in a chamber study of healthy humans. Inhal Toxicol 24:47–59. doi:10.3109/08958378.2011.633281

Stockfelt L, Sallsten G, Almerud P, Basu S, Barregard L (2013) Short-term chamber exposure to low doses of two kinds of wood smoke does not induce systemic inflammation, coagulation or oxidative stress in healthy humans. Inhal Toxicol 25:417–425. doi:10.3109/08958378.2013.798387

Stoeger T, Takenaka S, Frankenberger B, Ritter B, Karg E, Maier K, Schulz H, Schmid O (2009) Deducing in vivo toxicity of combustion-derived nanoparticles from a cell-free oxidative potency assay and metabolic activation of organic compounds. Environ Health Perspect 117:54–60. doi:10.1289/ehp.11370

Stohs SJ, Bagchi D (1995) Oxidative mechanisms in the toxicity of metal ions. Free Radic Biol Med 18:321–336

Straif K, Cohen A, Samet J (2013) IARC Scientific Publication No. 161

Swiston JR, Davidson W, Attridge S, Li GT, Brauer M, van Eeden SF (2008) Wood smoke exposure induces a pulmonary and systemic inflammatory response in firefighters. Eur Respir J 32:129–138. doi:10.1183/09031936.00097707

Tapanainen M, Jalava PI, Mäki-Paakkanen J, Hakulinen P, Happo MS, Lamberg H, Ruusunen J, Tissari J, Nuutinen K et al (2011) In vitro immunotoxic and genotoxic activities of particles emitted from two different small-scale wood combustion appliances. Atmos Environ 45:7546–7554. doi:10.1016/j.atmosenv.2011.03.065

Thurston GD, Ito K, Lall R (2011) A source apportionment of U.S. fine particulate matter air pollution. Atmos Environ 45:3924–3936. doi:10.1016/j.atmosenv.2011.04.070

Torvela T, Tissari J, Sippula O, Kaivosoja T, Leskinen J, Virén A, Lähde A, Jokiniemi J (2014a) Effect of wood combustion conditions on the morphology of freshly emitted fine particles. Atmos Environ 87:65–76. doi:10.1016/j.atmosenv.2014.01.028

Torvela T, Uski O, Karhunen T, Lähde A, Jalava P, Sippula O, Tissari J, Hirvonen M-R, Jokiniemi J (2014b) Reference particles for toxicological studies of wood combustion: formation, characteristics, and toxicity compared to those of real wood combustion particulate mass. Chem Res Toxicol 27:1516–1527. doi:10.1021/tx500142f

Totlandsdal AI, Låg M, Lilleaas E, Cassee F, Schwarze P (2015) Differential proinflammatory responses induced by diesel exhaust particles with contrasting PAH and metal content. Environ Toxicol 30:188–196. doi:10.1002/tox.21884

Uski O, Jalava PI, Happo MS, Leskinen J, Sippula O, Tissari J, Mäki-Paakkanen J, Jokiniemi J, Hirvonen M-R (2014) Different toxic mechanisms are activated by emission PM depending on combustion efficiency. Atmos Environ. doi:10.1016/j.atmosenv.2014.02.036

Val S, Stéphanie V, Martinon L, Laurent M, Cachier H, Hélène C, Yahyaoui A, Abderrazak Y, Marfaing H et al (2011) Role of size and composition of traffic and agricultural aerosols in the molecular responses triggered in airway epithelial cells. Inhal Toxicol 23:627–640. doi:10.3109/08958378.2011.599445

World Health Organization (WHO) (2014) Indoor air pollution and health, Fact sheet N292

Wu W, Bromberg PA, Samet JM (2013) Zinc ions as effectors of environmental oxidative lung injury. Free Radic Biol Med 65:57–69. doi:10.1016/j.freeradbiomed.2013.05.048